*Human Molecular Genetics, 2011, Vol. 20, No. 11* **2204–2212**
*doi:10.1093/hmg/ddr108*
*Advance Access published on March 22, 2011*

# Partial loss of *Tip60* slows mid-stage neurodegeneration in a spinocerebellar ataxia type 1 (SCA1) mouse model

**Kristin M. Gehrking[1,2], J. Michael Andresen[1,3], Lisa Duvick[1], John Lough[4], Huda Y. Zoghbi[5,6] and Harry T. Orr[1,2,3,*]**

[1]Institute of Human Genetics and Institute of Translational Neuroscience, [2]Department of Biochemistry, Biophysics and Molecular Biology and [3]Department of Laboratory Medicine and Pathology, University of Minnesota, Minneapolis, MN 55455, USA, [4]Department of Cell Biology, Neurobiology, and Anatomy, Medical College of Wisconsin, Milwaukee, WI 53226, [5]Department of Molecular and [6]Department of Human Genetics, Pediatrics, and Howard Hughes Medical Institute, Baylor College of Medicine, Houston, TX 77030, USA

Received October 11, 2010; Revised and Accepted March 11, 2011

**Spinocerebellar ataxia type 1 (SCA1) is one of nine dominantly inherited neurodegenerative diseases caused by polyglutamine tract expansion. In SCA1, the expanded polyglutamine tract is in the ataxin-1 (ATXN1) protein. ATXN1 is part of an *in vivo* complex with retinoid acid receptor-related orphan receptor alpha (Rora) and the acetyltransferase tat-interactive protein 60 kDa (Tip60). ATXN1 and Tip60 interact directly via the ATXN1 and HMG-box protein 1 (AXH) domain of ATXN1. Moreover, the phospho-mimicking Asp amino acid at position 776, previously shown to enhance pathogenesis, increases the ability of ATXN1 to interact with Tip60. Using a genetic approach, the biological relevance of the ATXN1/Tip60 interaction was assessed by crossing *ATXN1[82Q]* mice with *Tip60*$^{+/-}$ animals. Partial *Tip60* loss increased Rora and Rora-mediated gene expression and delayed ATXN1[82]-mediated cerebellar degeneration during mid-stage disease progression. These results suggested a specific, temporal role for Tip60 during disease progression. We also showed that genetic background modulated ATXN1[82Q]-induced phenotypes. Of interest, these latter studies showed that some phenotypes are enhanced on a mixed background while others are suppressed.**

## INTRODUCTION

Spinocerebellar ataxia type 1 (SCA1) is one of nine inherited polyglutamine diseases that cause neurodegeneration (1,2). In these diseases, the mutant gene encodes an expanded glutamine tract, which results in a polyglutamine expansion within the protein. In SCA1, the mutant *ATXN1* gene encodes the protein ataxin-1 (ATXN1), which is widely expressed (3,4); however, neurodegeneration is limited to cerebellar Purkinje cells, brainstem and spinal cord (5). As with most autosomal dominant ataxias, symptoms are characterized by a progressive loss of motor coordination, neuropathies, slurred speech, cognitive impairment and loss of other functional abilities arising from deep cerebellar nuclei (6).

Evidence indicates that a normal function of ATXN1 is to regulate gene expression. For example, ATXN1 interacts with a variety of transcription factors, including the zinc-finger transcription factors *Drosophila* Senseless and its mammalian homolog growth factor-independent 1 (7), the transcription corepressor silencing mediator of retinoid and thyroid hormone receptors (8), the human homolog of the *Drosophila* transcription repressor Capicua (9), the transcription factor Sp1 (10), the retinoid acid receptor-related orphan receptor alpha/tat-interactive protein 60 kDa (Rora/Tip60) complex (11) and the RNA-binding protein RBM17 (12). Moreover, ATXN1 contains a nuclear localization sequence (13). Wild-type (WT) ATXN1 shuttles between the nucleus and cytoplasm (14). Importantly, mutant ATXN1 must enter the nucleus to cause

*To whom correspondence should be addressed. Email: orrxx002@umn.edu

disease (13) and its nuclear export is greatly reduced (14). Within ATXN1 is the ATXN1 and HMG-box protein 1 (AXH) domain, a 120 amino acid stretch found in many proteins (15). The ATXN1 AXH domain crystal structure reveals an oligonucleotide-binding fold (16), which is likely the site of the proposed RNA-binding activity of ATXN1 (17).

Some of these ATXN1-interacting factors, in a dosage-dependent fashion, modify pathogenesis of SCA1 in mouse and fly models (7–9,11). Notably, *Rora* haploinsufficiency results in enhanced pathogenesis in SCA1 transgenic mice (11). Previous work demonstrates that in the murine cerebellum ATXN1, Tip60 and Rora exist in an endogenous complex. The ability of GST–ATXN1 bind to *in vitro* transcribed and translated Tip60 indicates that these proteins interact directly (11). To examine the biological import of the ATXN1/Tip60 interaction *in vivo*, we utilized a genetic approach to investigate the impact of *Tip60* haploinsufficiency in an SCA1 mouse model.

## RESULTS

### Mapping the Tip60-binding region of ATXN1

Previously using co-immunoprecipitations from WT cerebellar extracts, we showed that ATXN1, Rora and the coregulator Tip60 exist in a complex in which ATXN1 interacts directly with Tip60 (11). To examine the Tip60/ATXN1 interaction in more detail, a series of ATXN1 deletion constructs were generated and used in a GST-pull-down assay to assess their ability to interact with Tip60 (Fig. 1A). The results showed that an ATXN1 deletion construct that contained the AXH domain alone was sufficient to promote interaction with Tip60 (Fig. 1B, lane 9). In addition, all of the ATXN1 constructs containing the AXH domain [full length, full length without the self-association region (SAR) (18), fragment IV and fragment V] bound to Tip60 (Fig. 1B, lanes 3, 4, 6 and 7), while those lacking the AXH domain (fragment I and the SAR domain alone) did not bind Tip60 (Fig. 1B, lanes 5 and 8). Thus, we conclude that Tip60 binds to ATXN1 via the AXH domain.

Several lines of evidence indicate that phosphorylation of Ser776 is critical for the induction of neuronal dysfunction in SCA1 (12,19–21). Among these are data that a S776D substitution mimics phosphorylation and enhances disease severity (12,21). To examine whether D776 might also affect the interaction of ATXN1 with Tip60, GST pull-downs were performed using ATXN1–fragment V with either WT phosphorylatable Ser, phospho-resistant Ala or phospho-mimicking Asp at position 776. While substituting an Ala for the Ser at position 776 had no effect on the ability of ATXN1–fragment V to interact with Tip60, a phospho-mimicking Asp at residue 776 increased the ability of ATXN1–fragment V to interact with Tip60 (Fig. 1C), suggesting that the ATXN1/Tip60 interaction is modulated by S776 phosphorylation.

### *ATXN1*[*82Q*] mice with haploinsufficiency of *Tip60*

As a means to examine the biological relevance of the ATXN1/Tip60 complex, we used a genetic strategy to determine whether gene dosage impacts the SCA1 phenotype. The approach involved crossing $Tip60^{+/-}$ animals with *ATXN1*[*82Q*] mice from the B05 line in which an expanded *ATXN1* transgene is driven by the Purkinje cell protein 2 (*Pcp2/L7*) promoter (22). Heterozygous *Tip60* mice were generated using homologous recombination to replace exons 1–9 with a neomycin-targeting vector (23). Heterozygous mice with a null *Htatip* allele ($Tip60^{+/-}$) are viable and phenotypically normal. However, complete *Tip60* loss of function ($Tip60^{-/-}$) causes embryonic lethality near the blastocyst stage (23). The *Tip60* heterozygous mice were on the SV-129;C57BL/6 genetic background, and the *ATXN1*[82Q] mice were on the FVB background. Thus, offspring of this cross had genotypes of WT, *ATXN1*[*82Q*]:$Tip60^{+/-}$, *ATXN1*[*82Q*]:$Tip60^{+/+}$ and $Tip60^{+/-}$ all on a mixed FVB;SV-129;C57BL/6 background (Supplementary Material, Fig. S1A).

First, two crucial control analyses were performed. To confirm that $Tip60^{+/-}$ mice had a partial loss of function, we measured *Tip60* mRNA levels in cerebellar lysates. Heterozygous *Tip60* null mice expressed approximately half of WT *Tip60* levels (Supplementary Material, Fig. S1B). To assess whether partial *Tip60* loss affected *ATXN1*[*82Q*] transgene expression, we compared transgene expression between *ATXN1*[*82Q*] and *ATXN1*[*82Q*]:$Tip60^{+/-}$ mice. Since the expanded ATXN1[82Q] protein cannot be quantitatively solubilized from Purkinje cells of SCA1 transgenic mice (22), we used RNA levels to quantify transgene expression. By quantitative-PCR, *ATXN1* transgene expression was found to be similar regardless of *Tip60* gene dosage (Supplementary Material, Fig. S1C). In addition, ATXN1 immunostaining revealed no detectable difference in amount or deposition of ATXN1 in Purkinje cells between *ATXN1*[*82Q*] and *ATXN1*[*82Q*]:$Tip60^{+/-}$ mice (Supplementary Material, Figs S1D and S1E).

### Effect of genetic background on SCA1 phenotypes

Morphological and neurological assessments were used to examine the extent to which SCA1 phenotypes varied on the FVB and FVB;SV-129;C57BL/6 mixed backgrounds. Progressive thinning of the cerebellar molecular layer, reflecting Purkinje cell degeneration and dendritic tree atrophy, is a quantitative hallmark of pathology in the *Pcp2-SCA1* mice (21,24). To begin with, we determined the molecular layer thickness in WT-FVB and FVB;SV-129;C57BL/6 mice and whether it varied with age. WT-FVB cerebella had a relatively stable molecular layer thickness between 5 and 20 weeks of age. On the other hand, WT-FVB;SV-129;C57BL/6 mice had a slightly thinner molecular layer that decreased somewhat with age (Fig. 2A). Consistent with previous data (22,23,25), *ATXN1*[*82Q*] on an FVB background induced a slow, progressive Purkinje cell degeneration from 5 to 20 weeks of age. In contrast, the *ATXN1*[*82Q*]-FVB;SV-129;C57BL/6 mice had a slightly thinner molecular layer that decreased rapidly by 12 weeks of age and remained at 115 μM from 16 to 20 weeks of age (Fig. 2B).

Next, we assessed the motor phenotype using the accelerating rotarod paradigm. *ATXN1*[*82Q*] mice on the FVB genetic background showed a rotarod deficit as early as 5 weeks of age and had a more pronounced phenotype at 12 weeks (22,25). In contrast, *ATXN1*[*82Q*] mice on the FVB;SV-129;C57BL/6 genetic background (*ATXN1*[*82Q*]-*mix*) did not show a rotarod deficit until 30 weeks of age (Fig. 2C). Thus, while

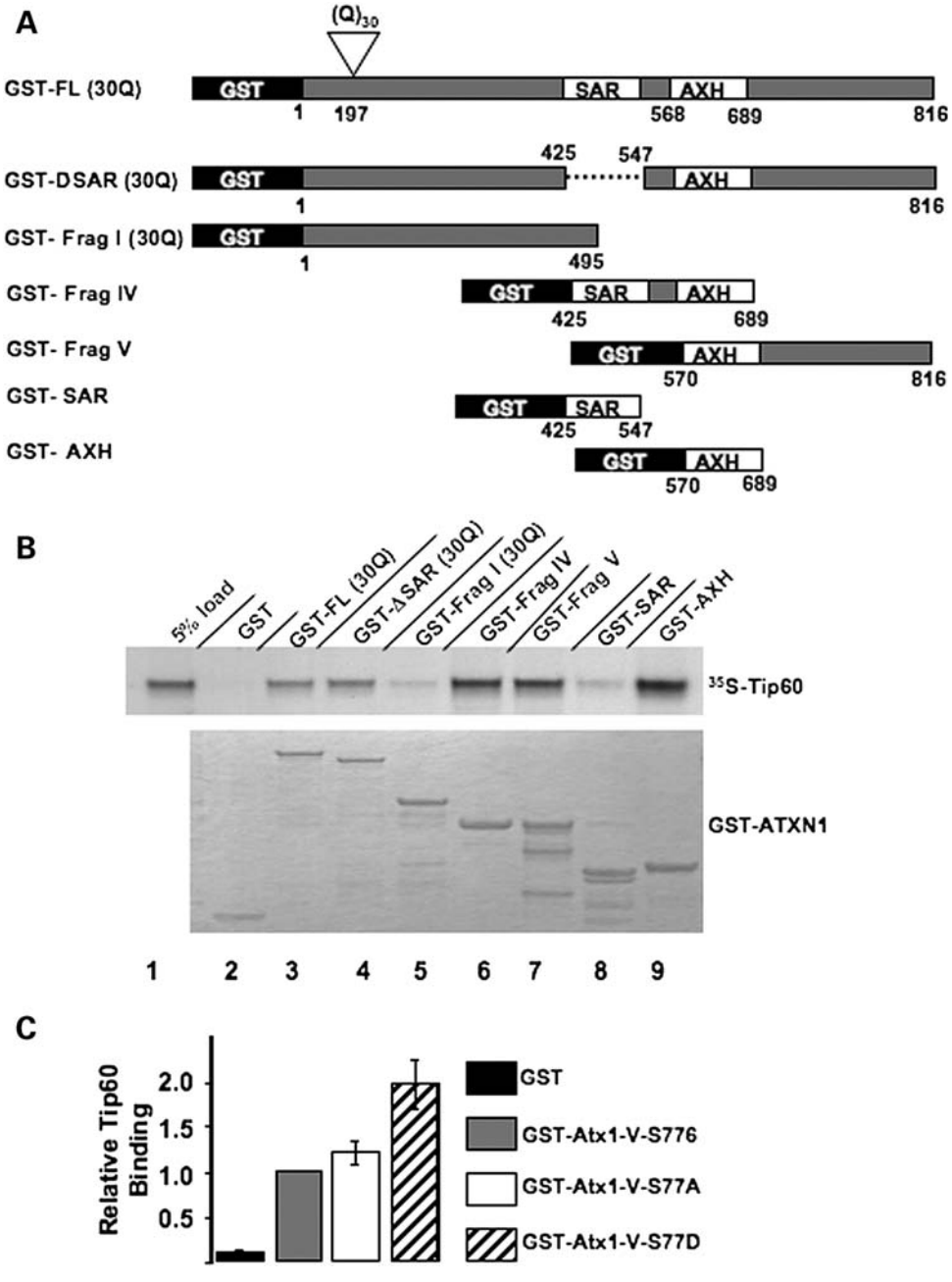


**Figure 1.** The interaction of ATXN1 with Tip60 requires the AXH domain of ATXN1 and is enhanced by a phospho-mimicking Asp at residue 776. (**A**) Diagrams of the GST–ATXN1 constructs used to pull-down His-tagged $^{35}$S-labeled Tip60. (**B**) Representative polyacrylamide gel showing the ability of GST–ATXN1 to pull-down His-tagged $^{35}$S-labeled Tip60. Upper panel depicts an autoradiograph of $^{35}$S-labeled Tip60 pulled down by each GST–ATXN1 construct. Lower panel shows Coomassie stained GST–ATXN1 constructs. (**C**) Quantification of Tip60 pulled down by GST–ATXN1–fragment V in which the amino acid at position 776 was either a Ser (S776), a phosphorylation resistant Ala (S776A) or phospho-mimicking Asp (S776D).

SCA1 molecular layer pathology was more pronounced on the mixed background, development of the neurological phenotype as determined by the rotarod was delayed in *ATXN1*[*82Q*]-*mix* mice.

### Partial loss of *Tip60* slows mid-stage ATXN1[82Q]-induced Purkinje cell pathology

To determine whether a partial loss of *Tip60* affected the SCA1 phenotype, several parameters were compared in WT, *ATXN1*[*82Q*] and *ATXN1*[*82Q*]*:Tip60*$^{+/-}$ mice all on the mixed FVB;SV-129;C57BL/6 background. We first examined the effect of *Tip60*$^{+/-}$ on SCA1 pathology *in vivo* by calbindin immunostaining and measurement of the molecular layer thickness (Fig. 3A). As quantified in Figure 3B, partial *Tip60* loss slowed neurodegeneration in *ATXN1*[*82Q*]*:Tip60*$^{+/-}$*-mix* mice relative to *ATXN1*[*82Q*]*-mix* mice during the mid-stage of disease. While the molecular layer was reduced in both *ATXN1*[*82Q*]*-mix* and *ATXN1*[*82Q*]*:Tip60*$^{+/-}$*-mix* mice at 5 weeks of age, at 12 and 16 weeks *ATXN1*[*82Q*]*:Tip60*$^{+/-}$*-mix*

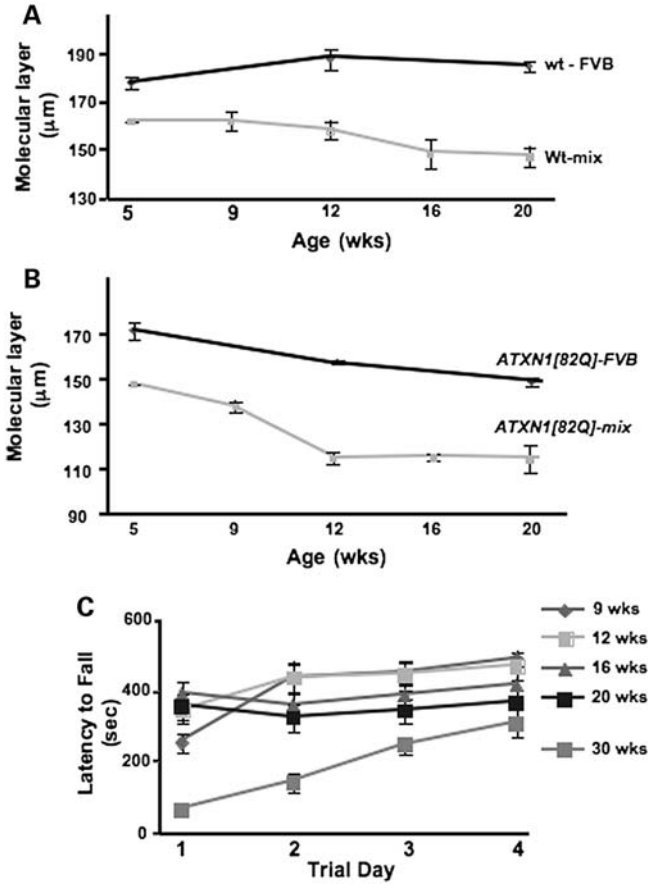


**Figure 2.** Genetic background affects SCA1 phenotypes in *ATXN1[82Q]* transgenic mice. (**A**) Cerebellar molecular layer thickness in aging WT-FVB and FVB;SV-129;C57BL/6 (mix) mice ($n = 3–7$ mice/genotype/age). (**B**) Cerebellar molecular layer thickness in aging FVB and FVB;SV-129;C57BL/6 (mix) mice expressing the *ATXN1[82Q]* transgene ($n = 3–7$ mice/genotype/age). (**C**) Motor performance using the accelerating rotarod paradigm in aging FVB;SV-129;C57BL/6 (mix) mice expressing the *ATXN1[82Q]* transgene ($n = 6–12$ mice/genotype).

cerebella had significantly thicker molecular layer than their *ATXN1*[*82Q*]-*mix* littermates. At 12 and 16 weeks, *ATXN1*[*82Q*]-*mix* mice had an average molecular layer thickness of 115 μM. In contrast, at 12 and 16 weeks, *ATXN1*[*82Q*]:*Tip60*$^{+/-}$-*mix* molecular layer thickness was 134 and 143 μM, respectively. At 20 weeks, *ATXN1*[*82Q*]:*Tip60*$^{+/-}$-*mix* molecular layer thickness thinned to 114 μM, identical to *ATXN1*[*82Q*]-*mix* littermates (115 μM, unchanged from 12 and 16 weeks) (Fig. 3B). Thus, partial loss of Tip60 resulted in a protective window between 12 and 16 weeks during which molecular layer thinning was slowed.

As an additional assessment of ATXN1[82Q]-induced pathology, we examined placement of excitatory synaptic terminals onto Purkinje cells in *SCA1* mice. Purkinje cells receive afferent, stimulatory input from climbing fibers expressing the glutamate transporter VGluT2 in their synaptic vesicles (26). Previously, we showed that the extension of climbing fiber terminals along the Purkinje cell dendritic tree is compromised in *ATXN1*[*82Q*]-*mix* mice (21). Using calbindin immunofluorescence to visualize Purkinje cell dendrites and VGluT2 immunofluorescence to visualize climbing fiber terminals, the extent of climbing fiber terminal extension along the Purkinje cell dendrites was measured in *ATXN1*[*82Q*]:*Tip60*$^{+/-}$-*mix* cerebella (Fig. 3C). At all ages, WT mice had a significantly greater climbing fiber extension along Purkinje cell dendrites compared with *ATXN1*[*82Q*]-*mix* expressing mice (Fig. 3D). However, at 12 and 16 weeks, partial loss of *Tip60* resulted in a reduction in the extent to which climbing fiber terminal extension was compromised by ATXN1[82Q]. At 12 and 16 weeks, *ATXN1*[*82Q*]:*Tip60*$^{+/-}$-*mix* mice had a significantly greater climbing fiber extension along Purkinje cell dendrites than their *ATXN1*[*82Q*]-*mix* littermates. By 20 weeks of age, extension of climbing fiber terminals in *ATXN1*[*82Q*]:*Tip60*$^{+/-}$-*mix* mice was as compromised as in *ATXN1*[*82Q*]-*mix* animals (Fig. 3D). Thus, by a second measure of ATXN1[82Q]-induced pathology, partial loss of *Tip60* afforded a protective period during the mid-stage, 12–16 weeks of age, of disease.

### Restoration of ATXN1[82Q]-induced changes in Rora, and Rora-mediated gene expression by a partial loss of *Tip60*

In *ATXN1*[*82Q*]-*mix* mice, mutant *ATXN1* depletes Rora from cerebellar Purkinje cells and *Ror*a haploinsufficiency results in enhanced pathogenesis in SCA1 transgenic mice (11). For the following set of experiments, we focused on a group of genes downregulated in both SCA1 and *staggerer* mice. Within this group, a subset of genes is known to bind Rora at the promoter (11,27–30). We sought to determine whether the protective effects on ATXN1[82Q]-induced pathology by *Tip60*$^{+/-}$ correlated with restoration of Rora and Rora-mediated gene expression.

Western blot analysis revealed that partial *Tip60* loss increased Rora protein expression relative to *ATXN1*[*82Q*]-*mix* littermates (Fig. 4A, lanes 3 versus 4). Next, we characterized the effect of partial *Tip60* loss on those Rora-mediated genes whose expression was previously found decreased in SCA1 and *staggerer* mouse cerebella (11). These include *Pcp2* (Purkinje cell protein 2), *Pcp4* (Purkinje cell protein 4), *Slc1a6* (solute carrier family 1-high affinity aspartate/glutamate transporter 6) and *Itpr1* (Inositol 1,4,5-triphosphate receptor, type 1). Gene expression was assessed at three ages: 8 weeks, an early stage with intermediate Purkinje cell atrophy; 12 weeks, mid-stage during the period of the *Tip60*$^{+/-}$-induced protection; and 20 weeks, late stage when both *ATXN1*[*82Q*]-*mix* and *ATXN1*[*82Q*]:*Tip60*$^{+/-}$-*mix* Purkinje cell atrophy reached the same advanced level. At all ages, WT-mix and *Tip60*$^{+/-}$-mix gave the same results (data not shown).

In 8-week-old mice, there were no significant differences between WT-mix, *ATXN1*[*82Q*]-*mix* and *ATXN1*[*82Q*]:*Tip60*$^{+/-}$-*mix* expression of *Slc1a6*, *Pcp4, Pcp2* or *Itpr1*

**Figure 3.** *Tip60* haploinsufficiency rescues SCA1 cerebellar pathology during the mid-stage of disease. (**A**) Calbindin immunofluorescence of Purkinje cells in aging WT, *ATXN1[82Q]* and *ATXN1[82Q]:Tip60*$^{+/-}$ FVB;SV-129;C57BL/6 (mix) mice. (**B**) Quantitative analysis of the molecular thickness in aging WT, *ATXN1[82Q]* and *ATXN1[82Q]:Tip60*$^{+/-}$ FVB;SV-129;C57BL/6 (mix) mice ($n = 3–7$ mice/genotype/age). (**C**) Immunofluorescence of calbindin (red) and VGluT2 (green) in WT, *ATXN1[82Q]* and *ATXN1[82Q]:Tip60*$^{+/-}$ FVB;SV-129;C57BL/6 (mix) mice. (**D**) Quantitative analysis of the climbing fiber extension along Purkinje cell dendrites in aging WT, *ATXN1[82Q]* and *ATXN1[82Q]:Tip60*$^{+/-}$ FVB;SV-129;C57BL/6 (mix) mice ($n = 3–5$ mice/genotype/age).

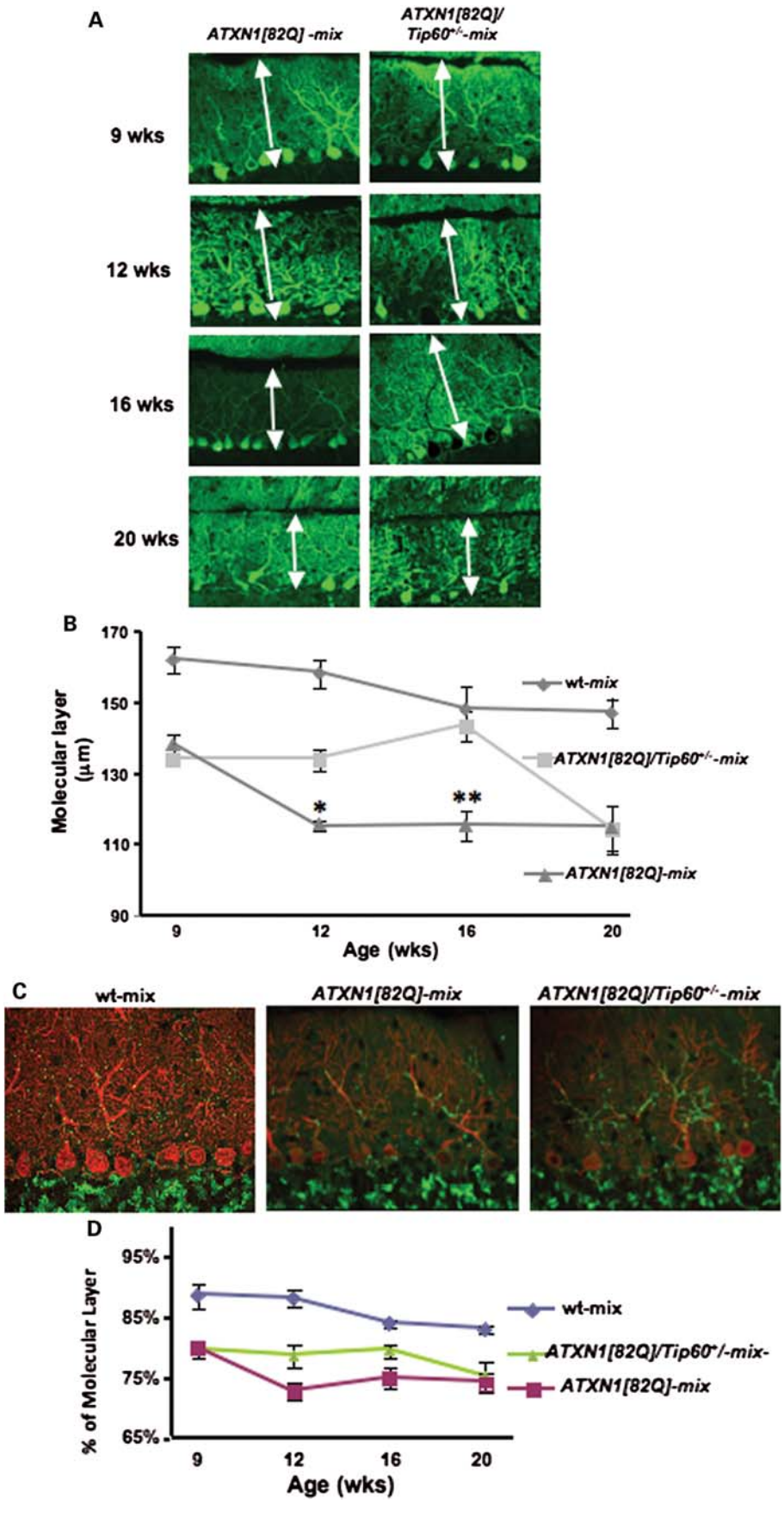
A
ATXN1[82Q] -mix
ATXN1[82Q]/ Tip60+/--mix
9 wks
12 wks
16 wks
20 wks
B
Molecular layer (μm)
170
150
130
110
90
9
12
16
20
Age (wks)
wt-mix
ATXN1[82Q]/Tip60+/--mix
ATXN1[82Q]-mix
*
**
C
wt-mix
ATXN1[82Q]-mix
ATXN1[82Q]/Tip60+/--mix
D
% of Molecular Layer
95%
85%
75%
65%
9
12
16
20
Age (wks)
wt-mix
ATXN1[82Q]/Tip60+/-mix-
ATXN1[82Q]-mix

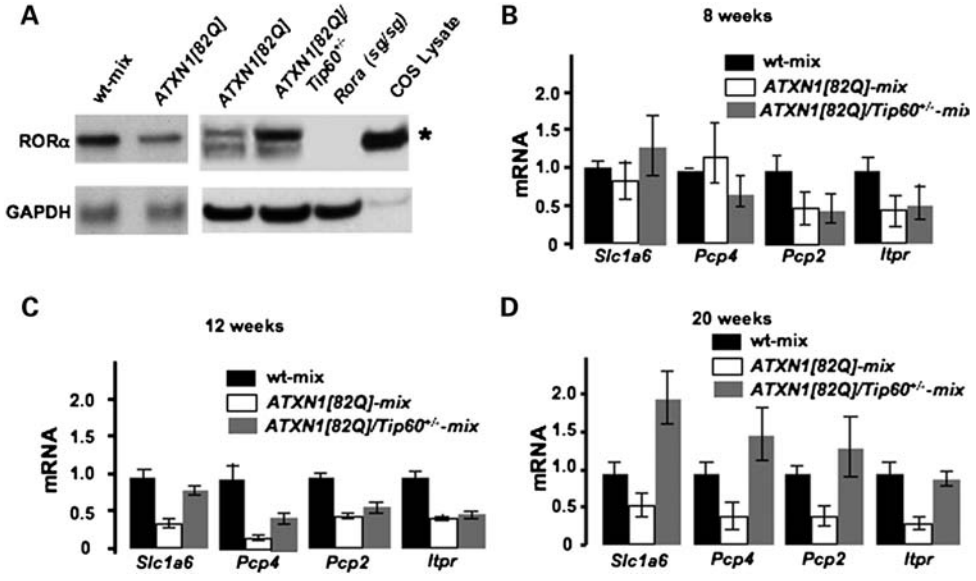


**Figure 4.** *Tip60* haploinsufficiency restoration of Rora levels ($n = 3$ mice) and Rora-mediated gene expression. (**A**) Western blot analysis of cerebellar Rora levels in WT, *ATXN1[82Q]* and ATXN1[82Q]:Tip60$^{+/-}$ FVB;SV-129;C57BL/6 (mix) mice, and in homozygous staggerer (*sg/sg*) mice at 12 weeks of age. COS cells transfected with *Rora* cDNA are shown as a positive control. (**B**) Quantitative PCR of four Rora-mediated genes in WT, *ATXN1[82Q]* and *ATXN1[82Q]:Tip60*$^{+/-}$ FVB;SV-129;C57BL/6 (mix) mice at 8 weeks of age. (**C**) Quantitative PCR of four Rora-mediated genes in WT, *ATXN1[82Q]* and *ATXN1[82Q]Tip60*$^{+/-}$ FVB;SV-129;C57BL/6 (mix) mice at 12 weeks of age. (**D**) Quantitative PCR of four Rora-mediated genes in WT, *ATXN1[82Q]* and *ATXN1[82Q]:Tip60*$^{+/-}$ FVB;SV-129;C57BL/6 (mix) mice at 20 weeks of age.

(Fig. 4B). At 12 weeks, *Slc1a6* and *Pcp4* expression were significantly higher in *ATXN1*[*82Q*]*:Tip60*$^{+/-}$*-mix* mice compared with *ATXN1*[*82Q*]*-mix* mice (Fig. 4C). At 20 weeks in addition to *Slc1a6* and *Pcp4* expression, *Itpr1* was also significantly higher in *ATXN1*[*82Q*]*:Tip60*$^{+/-}$ than *ATXN1*[*82Q*] mice (Fig. 4D). Interestingly, *Slca6* expression at 20 weeks was significantly higher than in WT-mix cerebella. Thus, in the presence of ATXN1[82Q] and with increasing age, the expression of at least some Rora-mediated genes become abnormally elevated in *Tip60* haploinsufficient mice. We also examined the expression of three SCA1/*staggerer* downregulated Rora-mediated genes (*Calb1*, *Idb2* and *Cals*) at 20 weeks of age, which had previously been shown to not have Tip60 at the promoter complex (29). This is in contrast to Slca6 and Pcp4, which have Rora-dependent recruitment of Tip60 to the promoter complex (29). In each case, expression was not restored in *ATXN1*[*82Q*]*:Tip60*$^{+/-}$*-mix* mice compared with *ATXN1*[*82Q*]*-mix* mice (Supplementary Material, Fig. S2).

## DISCUSSION

Previously, we showed that ATXN1, Rora and the coregulator Tip60 exist in a complex in which ATXN1 interacts directly with Tip60 (11). In the present study, we further examined the interaction of ATXN1 and Tip60, showing that this interaction is both dependent on ATXN1's AXH domain and enhanced by a phospho-mimicking Asp at position 776. Importantly, the AXH domain is required for mutant, polyglutamine-containing ATXN1 to induce neurodegeneration (7). Recently, we showed that a phospho-mimicking Asp at residue 776 enhances ATXN1-induced pathogenesis (21). Thus, Tip60 interacts with a region of ATXN1 crucial for disease, and this interaction is promoted by an amino acid substitution that enhances pathogenesis. Moreover, the finding that D776 promotes the ATXN1/Tip60 interaction strengthens the concept that the conformational change induced by S776 phosphorylation includes the AXH domain. Based on these features, we hypothesized that the ATXN1/Tip60 interaction has biological relevance.

As a basis for examining the ATXN1/Tip60 interaction *in vivo*, we reasoned that reducing Tip60 levels might modify ATXN1[82Q]-induced disease. We found that a partial loss of *Tip60* slowed the progression of ATXN1[82Q]-induced Purkinje cell atrophy. The protective effect of reduced *Tip60* levels was associated with increased Rora protein and Rora-mediated gene expression. These results indicate that Tip60-mediated pathways contribute to SCA1.

By two measures of pathology, we found Purkinje cell degeneration was slowed in *ATXN1*[*82Q*]*:Tip60*$^{+/-}$*-mix* compared with *ATXN1*[*82Q*]*-mix* animals. The protective effect of a partial loss of *Tip60* was restricted to the period between 12 and 16 weeks of age, i.e. a mid-stage of disease progression in this model of Purkinje cell disease in SCA1. The observation that *Tip60*$^{+/-}$ seems not to have affected disease onset and that its protective effect diminished with age raises some interesting points. First, the lack of a *Tip60*$^{+/-}$ effect on early disease suggests that the ATXN1/Tip60 interaction does not impact ATXN1's postulated role in Purkinje cell development and disease onset (11). Rather, the data suggest that the interaction of mutant ATXN1 with Tip60 plays a role in SCA1 progression after disease initiation. The pattern of *Tip60*$^{+/-}$ protective effect adds to the concept that disease initiation and progression result from mutant ATXN1's effects on various and complex cellular pathways. The *Tip60*$^{+/-}$ protective window corresponds to the time period previously shown

to separate disease initiation and neuronal dysfunction from subsequent Purkinje cell death (21), suggesting that perhaps the pathways critical for progression to neuronal death overlap with those that limit the extent of the *Tip60*$^{+/-}$ protective effect.

The pattern of the *Tip60*$^{+/-}$ effect on Rora-mediated gene expression illustrates the complex role of this system in SCA1. Both Rora and Rora-mediated gene expression are decreased in ATXN1[82Q] mutant mice (11). Consistent with Rora's role in SCA1 pathogenesis, the ATXN1[82Q]-induced loss of Rora was reversed at 12 weeks of age in *ATXN1*[*82Q*]:*Tip60*$^{+/-}$*-mix* animals. Moreover, *Tip60*$^{+/-}$ was also associated with a restoration of certain Rora-mediated genes at 12 weeks of age. Interestingly, not all Rora-mediated gene expression levels were restored by partial *Tip60* loss at 12 weeks of age. However, by 20 weeks of age, expression of all four Rora-mediated genes examined was at or above the WT level. Thus, the restoration of some Rora-mediated genes (e.g. *Slc1a6* and *Pcp4*) occurred early in the *Tip60*$^{+/-}$ protective window, while the restoration of others was delayed (e.g. *Pcp2* and *Itpr1*). This suggests that only a subset of Rora-mediated genes may contribute to the *Tip60*$^{+/-}$ protective effect. It is important to note that *Pcp4* and *Slc1a6* are not only genes with Rora-mediated expression, but are also genes with Rora-dependent recruitment of Tip60 to the promoter complex (29). Conversely, the expression of three genes examined that did not show significant changes in *ATXN1*[*82Q*]*;Tip60*$^{+/-}$ mice (*Calb1*, *Grm1* and *Cals*) are genes where Rora does not recruit Tip60 to the transcription complex (29). Interestingly, expression of all of the four Rora-mediated genes that were elevated in *ATXN1*[*82Q*]*:Tip60*$^{+/-}$ mice remained elevated at 20 weeks of age when *Tip60*$^{+/-}$ was no longer protective. Perhaps in these mice, overexpression of certain Rora-mediated genes, e.g. *Slc1a6*, contributes to toxicity.

Whether partial *Tip60* loss enhances Rora-mediated gene expression by relieving ATXN1-induced Rora depletion or perhaps alters specific posttranslational modifications that impact Rora-mediated transcription remains an open question. Tip60 was shown to be a co-activator for the androgen nuclear receptor (32). Moreover, androgen receptor activation by Tip60 acetylation requires direct interaction via Tip60's LXXL motif (33). It is intriguing to speculate that perhaps the acetyltransferase activity of Tip60 is in some way connected to the decrease in cerebellar Rora induced by ATXN1[82Q]. If this were to be the case, this would support a model where the function of Tip60, coactivator versus corepressor, varies depending on the nuclear receptor and other proteins with which it associates.

Our results also showed that the time course and severity of SCA1 symptoms in the mouse varied when the same mutant *ATXN1*[*82Q*] transgene was expressed on two different genetic backgrounds. Purkinje cell degeneration was more rapid when *ATXN1*[*82Q*] was expressed on the mixed genetic background versus the FVB background. Moreover, development of motor performance deficit (ataxia) was delayed on the mixed background compared with the FVB background. This strongly suggests the presence of genetic modifiers regulating the severity of SCA1 phenotypes in mice. Disease presentation in SCA1 patients is also greatly influenced by non-polyglutamine factors, which may include genetic modifiers (34,35). Identifying the genetic modifiers that influence SCA1 phenotypes in mice should illuminate additional pathways that influence neurodegeneration.

In summary, we conclude the ATXN1/Tip60 interaction contributes to SCA1 pathogenesis with a partial loss of *Tip60* delaying cerebellar degeneration in an SCA1 mouse model, specifically during mid-stage disease. These findings, taken with the observation that ATXN1[82Q]-mediated pathology and ATXN1[82Q]-mediated motor deficits are differentially influenced by genetic background, indicate that not only is the relationship between the molecular pathways that underlie disease initiation and progression complex, so is the relationship between pathology and neuronal dysfunction.

## MATERIALS AND METHODS

### *In vitro* transcription/translation GST pull-down assay

*ATXN1* cDNAs were cloned into pGEX vectors (Amersham Biosciences) and expressed in *E. coli* BL21(DE3) cells. Human *Tip60* was cloned into pCDNA3.1/His expression vector (Invitrogen). *In vitro* transcription/translation and GST pull-down were done as described (11). Samples were run on NuPage 4–12% Bis–Tris polyacrylamide gels (Invitrogen), stained with SimplyBlue SafeStain colloidal Coomassie (Invitrogen) and dried on Whatman 3MM paper. Amount of ATXN1 was measured by densitometry of the Coomassie staining, and bound radioactive Tip60 was determined by autoradiography followed by band excision and scintillation counting.

### Mouse genotyping

*Animal breeding*. WT, *Tip60*$^{+/-}$, *ATXN1*[*82Q*] and *ATXN1*[*82Q*]*:Tip60*$^{+/-}$ mice were the $F_1$ progeny (1:1:1:1) resulting from breeding *ATXN1*[*82Q*] and *Tip60*$^{+/-}$ mice. *ATXN1*[*82Q*] mice were maintained on the FVB background and the *Tip60*$^{+/-}$ mice on a SV-129;C57BL/6 background.

*Genotyping of mice*. PCR was used to identify *Tip60*$^{+/-}$ and *ATXN1*[*82Q*] transgenic animals as described by Hu *et al*. (23) and Burright *et al*. (22), respectively.

### Immunostaining and quantitative measurements

Animals were perfused with 10% formalin and 50 micron vibratome sections cut as described (21). Floating cerebellar slices were incubated with the following primary antibodies in blocking buffer [2% donkey serum, 0.3% Triton X-100 in 1× phosphate buffered saline (PBS)] at dilutions indicated: goat calbindin (SC-7691, Santa Cruz Biotechnology) at 1:500, rabbit 11750/ataxin-1 at 1:2500 and mouse VGLUT2 (MAB5504, Millipore) at 1:1000. Secondary antibodies used were: donkey anti-goat Cy3 (#705-165-147, Jackson Immunoresearch) at 1:500, donkey anti-rabbit Cy2 (#711-225-152, Jackson Immunoresearch) at 1:500 and donkey anti-mouse Cy5 (#115-175-146, Jackson Immunoresearch) at 1:500. Sections were washed, mounted onto microscope slides with glycerol–gelatin containing 4 mg/ml *n*-proplyl gallate (Sigma)

and visualized on a FluoView inverted confocal, laser-scanning microscope (#FV1000 IX2, Olympus). Molecular layer thickness was measured with FluoView software.

For molecular layer measurements, calbindin-stained Purkinje cells were analyzed from two sagittal sections that were analyzed per mouse from at least five mice per genotype. Using confocal laser-scanning microscopy, six measurements were taken at the primary fissure and averaged to determine molecular layer thickness (21,24). For climbing fiber-Purkinje cell measurements, climbing fibers were similarly measured with VGluT2 antibody staining from six measurements at the primary fissures of two sagittal sections per mouse in at least three mice per genotype. Purkinje cell dendrite lengths were obtained as stated above, and the climbing fiber:Purkinje cell ratio was calculated with averaged measurements. Data are expressed as the mean ± SEM. The *P*-value was calculated using Student's *t*-test (two-tailed equal variance).

### Gait analysis

Accelerating Rotarod (Model 7650 Ugo Basile) analysis was performed at 9, 12, 16, 20 and 30 weeks of age as described (25). Student's *t*-test was used to assess statistical significance.

### Western blot analysis

Mouse cerebella were homogenized in brain extraction buffer: 0.25 M Tris–HCl pH 7.5 with phosphatase inhibitors cocktails I and II (P2850, P5726 Sigma) and protease inhibitors (1183617001, Roche). Forty milligrams of protein were denatured, run on 4–12% Bis–Tris Gel (NP0321BOX, Invitrogen) and blotted on nitrocellulose membrane (Protran BA 85, Whatman/GE Healthcare). Membranes were blocked overnight at 4°C with 10% blotto (10% w/v milk in 1× tris buffered saline) with 0.1% v/v Tween-20. Blocked membranes were incubated with RORα antibody (H-65 #sc-28612, Santa Cruz Biotechnology) for 1 h at 22°C, washed three times with 0.1% PBS + 0.1% tween and incubated with anti-goat horse radisn peroxidase secondary antibody for 45 min. Samples were probed with mouse anti-GAPDH (#MAB374, Chemicon) as a loading control. Densitometry was used to quantify protein levels.

### Quantitative RT–PCR

Total RNA was isolated from the cerebella of *ATXN1*[*82Q*], *ATXN1*[*82Q*]*:Tip60*$^{+/-}$ and WT littermates at 8, 12 and 20 weeks using the TRIZOL method (Invitrogen). A minimum of three mice was used per genotype. Fifty nanograms of total RNA were used per reaction in triplicate with the TaqMan one-step reverse transcriptase (RT)–PCR kit (#4309169, Applied Biosytems). The following probes were assayed from Applied Biosystems: *Pcp2* (Mm00435514_m1), *Pcp4* (Mm00500973_m1), *Slc1a6* (Mm00436591_m1) and *Itpr1* (Mm01183049_m1). Samples were normalized to GAPDH. Reactions were run on a Real-time Quantitative PCR System ABI PRISM 7500.

### Cell culture

*Cell growth and transfection*. For Rora experiments, CHO cells were grown in Gibco™ Minimum Essential Medium (MEM) and Alpha Medium (#32561037, Invitrogen) supplemented with 10% FBS and Pen/strep. Cells were plated in media without antibiotics 24 h before transfection at $10^5$ cells/ml unless otherwise specified. Cells were transfected with Lipofectamine Plus (#11514-015, Invitrogen).

*Cell culture lysates*. At 48 h post-transfection, cells were lysed in Tris-Triton lysis buffer (50 mM Tris–HCl pH 7.5, 2.5 mM $MgCl_2$, 100 mM NaCl, 0.5% Triton), with phosphatase inhibitors, protease inhibitors and sodium butyrate. Protein was run on 4–12% Bis–Tris gels.

### Statistical analysis

Data were expressed as the mean ± standard error of the mean. Statistical comparisons were made with student's *t*-test unless otherwise noted.

## SUPPLEMENTARY MATERIAL

Supplementary Material is available at *HMG* online.

## ACKNOWLEDGEMENTS

We are grateful to Robert Ehlenfeldt and Orion Rainwater for managing the SCA1 mouse colony.

*Conflict of Interest statement*. None declared.

## FUNDING

This work was supported by National Institutes of Health grants (NS022920, H.T.O.) and (NS055409, K.M.G.). Funding to pay the Open Access publication charges for this article was provided by a Ruth L. Kirschstein NRSA to K.M.G.

## REFERENCES

1. Orr, H.T., Chung, M.Y., Banfi, S., Kwiatkowski, T.J. Jr, Servadio, A., Beaudet, A.L., McCall, A.E., Duvick, L.A., Ranum, L.P. and Zoghbi, H.Y. (1993) Expansion of an unstable trinucleotide CAG repeat in spinocerebellar ataxia type 1. *Nat. Genet.*, **4**, 221–226.
2. Orr, H.T. and Zoghbi, H.Y. (2007) Trinucleotide repeat disorders. *Ann. Rev. Neurosci.*, **30**, 575–621.
3. Servadio, A., Koshy, B., Armstrong, D., Antalffy, B., Orr, H.T. and Zoghbi, H.Y. (1995) Expression analysis of the ataxin-1 protein in tissues from normal and spinocerebellar ataxia type 1 individuals. *Nat. Genet.*, **10**, 94–98.
4. Banfi, S., Servadio, A., Chung, M., Capozzoli, F., Duvick, L.A., Elde, R., Zoghbi, H.Y. and Orr, H.T. (1996) Cloning and developmental expression analysis of the murine homolog of the spinocerebellar ataxia type 1 gene (Sca1). *Hum. Mol. Genet.*, **5**, 33–40.
5. Koeppen, A.H. (2005) The pathogenesis of spinocerebellar ataxia. *Cerebellum*, **4**, 62–73.
6. Zoghbi, H.Y. (1995) Spinocerebellar ataxia type 1. *Clin. Neurosci.*, **3**, 5–11.
7. Tsuda, H., Jafar-Nejad, H., Patel, A.J., Sun, Y., Chen, H.K., Rose, M.F., Venken, K.J., Botas, J., Orr, H.T., Bellen, H.J. *et al.* (2005) The AXH domain of Ataxin-1 mediates neurodegeneration through its interaction with Gfi-1/senseless proteins. *Cell*, **122**, 633–644.

8. Mizutani, A., Wang, L., Rajan, H., Vig, P., Alaynick, W., Thaler, J. and Tsai, C.-C. (2005) Boat, an AXH domain protein, suppresses the cytotoxicity of mutant ataxin-1. *EMBO J.*, **24**, 3339–3351.
9. Lam, Y.C., Bowman, A.B., Jafar-Nejad, P., Lim, J., Richman, R., Fryer, J.D., Hyun, E.D., Duvick, L.A., Orr, H.T., Botas, J. *et al.* (2006) ATAXIN-1 interacts with the repressor Capicua in its native complex to cause SCA1 neuropathology. *Cell*, **127**, 1335–1347.
10. Goold, R., Hubank, M., Hunt, A., Holton, J., Menon, R.P., Revesz, T., Pandolfo, M. and Matilla-Duenas, A. (2007) Down-regulation of the dopamine receptor D2 in mice lacking ataxin 1. *Hum. Mol. Genet.*, **16**, 2122–2134.
11. Serra, H.G., Duvick, L., Zu, T., Carlson, K., Stevens, S., Jorgensen, N., Lysholm, A., Burright, E., Zoghbi, H.Y., Clark, H.B. *et al.* (2006) RORalpha-mediated Purkinje cell development determines disease severity in adult SCA1 mice. *Cell*, **127**, 697–708.
12. Lim, J., Crespo-Barreto, J., Jafar-Nejad, P., Bowman, A.B., Richman, R., Hill, D.E., Orr, H.T. and Zoghbi, H.Y. (2008) Opposing effects of polyglutamine expansion on native protein complexes contribute to SCA1. *Nature*, **452**, 713–719.
13. Klement, I.A., Skinner, P.J., Kaytor, M.D., Yi, H., Hersch, S.M., Clark, H.B., Zoghbi, H.Y. and Orr, H.T. (1998) Ataxin-1 nuclear localization and aggregation: role in polyglutamine-induced disease in *SCA1* transgenic mice. *Cell*, **95**, 41–53.
14. Irwin, S., Vandelft, M., Howell, J.L., Graczyk, J., Orr, H.T. and Truant, R. (2005) RNA association and nucleocytoplasmic shuttling by ataxin-1. *J. Cell Sci.*, **118**, 233–242.
15. de Chiara, C., Giannini, C., Adinolfi, S., de Boer, J., Guida, A., Ramos, A., Jodice, C., Kioussis, D. and Pastore, A. (2003) The AXH module: an independently folded domain common to ataxin-1 and HBP1. *FEBS Lett.*, **551**, 107–112.
16. Chen, Y.W., Allen, M.D., Veprintsev, D.B., Lowe, J. and Bycroft, M. (2004) The structure of the AXH domain of spinocerebellar ataxin-1. *J. Biol. Chem.*, **279**, 3758–3765.
17. Yue, S., Serra, H.G., Zoghbi, H.Y. and Orr, H.T. (2001) The spinocerebellar ataxia type 1 protein, ataxin-1, has RNA-binding activity that is inversely affected by the length of its polyglutamine tract. *Hum. Mol. Genet.*, **10**, 25–30.
18. Burright, E.N., Davidson, J.D., Duvick, L.A., Koshy, B., Zoghbi, H.Y. and Orr, H.T. (1997) Identification of a self-association region within the SCA1 gene product, ataxin-1. *Hum. Mol. Genet.*, **6**, 513–518.
19. Chen, H.-K., Fernandez-Funez, P., Acevedo, S.F., Lam, Y.C., Kaytor, M.D., Fernandez, M.H., Aitken, A., Skoulakis, E.M.C., Orr, H.T., Botas, J. *et al.* (2003) Interaction of Akt-phosphorylated ataxin-1 with 14-3-3 mediates neurodegeneration in spinocerebellar ataxia type 1. *Cell*, **113**, 457–468.
20. Emamian, E.S., Kaytor, M.D., Duvick, L.A., Zu, T., Tousey, S.K., Zoghbi, H.Y., Clark, H.B. and Orr, H.T. (2003) Serine 776 of ataxin-1 is critical for polyglutamine-induced disease in SCA1 transgenic mice. *Neuron*, **38**, 375–387.
21. Duvick, L., Barnes, J., Ebner, B., Agrawal, S., Andresen, M., Lim, J., Giesler, G.J., Zoghbi, H.Y. and Orr, H.T. (2010) SCA1-like disease in mice expressing wild type ataxin-1 with a serine to aspartic acid replacement at residue 776. *Neuron*, **67**, 929–935.
22. Burright, E.N., Clark, H.B., Servadio, A., Matilla, T., Feddersen, R.M., Yunis, W.S., Duvick, L.A., Zoghbi, H.Y. and Orr, H.T. (1995) SCA1 transgenic mice: a model for neurodegeneration caused by an expanded CAG trinucleotide repeat. *Cell*, **82**, 937–948.
23. Hu, Y., Fisher, J.B., Kopprowski, S., McAllister, D., Kim, M.-S. and Lough, J. (2009) Homozygous disruption of the *Tip60* gene causes early embryonic lethality. *Develop. Dynam.*, **238**, 2912–2921.
24. Zu, T., Duvick, L.A., Kaytor, M.D., Berlinger, M.S., Zoghbi, H.Y., Clark, H.B. and Orr, H.T. (2004) Recovery from polyglutamine-induced neurodegeneration in conditional SCA1 transgenic mice. *J. Neurosci.*, **24**, 8853–8861.
25. Clark, H.B., Burright, E.N., Yunis, W.S., Larson, S., Wilcox, C., Hartman, B., Matilla, A., Zoghbi, H.Y. and Orr, H.T. (1997) Purkinje cell expression of a mutant allele of SCA1 in transgenic mice leads to disparate effects on motor behaviors, followed by a progressive cerebellar dysfunction and histological alterations. *J. Neurosci.*, **17**, 7385–7395.
26. Fremeau, R.T., Troyer, M.D., Pahner, I., Nygaard, G.O., Tran, C.H., Reimer, R.J., Bellocchio, E.E., Fortin, D., Storm-Mathisen, J. and Edwards, R.H. (2001) The expression of vesicular glutamate transporters defines two classes of excitatory synapse. *Neuron*, **31**, 247–260.
27. Sidman, R.L., Lane, P.W. and Dickie, M.M. (1962) Staggerer, a new mutation in the mouse affecting the cerebellum. *Science*, **137**, 610–612.
28. Hamilton, B.A., Frankel, W.N., Kerrebrock, A.W., Hawkins, T.L., FitzHugh, W., Kusumi, K., Russell, L.B., Mueller, K.L., van Berkel, V., Birren, B.W. *et al.* (1996) Disruption of the nuclear hormone receptor RORalpha in staggerer mice. *Nature*, **379**, 736–739.
29. Gold, D.A., Baek, S.H., Schork, N.J., Rose, D.W., Larsen, D.D., Sachs, B.D., Rosenfeld, M.G. and Hamilton, B.A. (2003) RORalpha coordinates reciprocal signaling in cerebellar development through sonic hedgehog and calcium-dependent pathways. *Neuron*, **40**, 1119–1131.
30. Crespo-Barreto, J.M., Fryer, J.D., Shaw, C.A., Orr, H.T. and Zoghbi, H.Y. (2010) Partial loss of ataxin-1 function contributes to transcriptional dysregulation in spinocerebellar ataxia type 1 pathogenesis. *PLoS Genet.*, **6**, e1001021.
31. Utley, R.T. and Cote, J. (2003) The MYST family of histone acetyltransferases. *Curr. Top. Microbiol. Immunol.*, **274**, 203–236.
32. Brady, M.E., Ozanne, D.M., Gaughan, L., Waite, I., Cook, S., Neal, D.E. and Robson, C.N. (1999) Tip60 is a nuclear hormone receptor coactivator. *J. Biol. Chem.*, **274**, 17599–17604.
33. Gaughan, L., Logan, I.R., Cook, S., Neal, D.E. and Robson, C.N. (2002) Tip60 and histone deacetylase 1 regulate androgen receptor activity through changes to the acetylation status of the receptor. *J. Biol. Chem.*, **277**, 25904–25913.
34. Globas, C., du Montcel, S.T., Baliko, L., Boesch, S., Depondt, C., DiDonato, S., Durr, A., Filla, A., Klockgetheer, T., Mariotti, C. *et al.* (2008) Early symptoms in spinocerebellar ataxia type 1, 2, 3, and 6. *Mov. Disord.*, **23**, 2232–2238.
35. van de Warrenburg, B.P., Hendriks, H., Dürr, A., van Zuijlen, M.C., Stevanin, G., Camuzat, A., Sinke, R.J., Brice, A. and Kremer, B.P. (2005) Age at onset variance analysis in spinocerebellar ataxias: a study in a Dutch-French cohort. *Ann. Neurol.*, **57**, 505–512.